Examining runoff generation processes in the Selke catchment in central Germany: Insights from data and semi-distributed numerical model

Sumit Sinha [a,b,*], Michael Rode [b], Dietrich Borchardt [b]

[a] Geography Department, Durham University, Science Site, Durham, DH1 3LE, UK
[b] Department of Aquatic Ecosystem Analysis, Helmholtz Centre for Environmental Research-UFZ, Bruckstrasse 3a, 39114 Magdeburg, Germany

ARTICLE INFO

ABSTRACT

Study region: Our study is focussed on a mesoscale catchment, Selke, in central Germany having an area of 463 km^2 with spatially diverse land-use from upland to the low-lying areas in the vicinity of the catchment outlet.

Study focus: This study used rainfall-runoff data available on daily time step to examine the spatio-temporal variation of runoff coefficients. We then applied a validated semi-distributed hydrological model, HYPE, for examining the spatio-temporal variation of runoff generating mechanisms. HYPE model was modified in a minor fashion and simulations were conducted again to find out the portion of discharge originating from different runoff generation mechanisms.

New hydrological insights for the region: We examined the spatio-temporal variation of runoff generating mechanisms on the sub-basin level on seasonal basis. Our analysis reveals that the runoff generation in the Selke catchment is primarily dominated by shallow sub-surface flow and very rarely the contribution from Dunne overland flow exceeds sub-surface flow. Runoff generated by Hortonian mechanism is very infrequent and almost negligible. We also examined the spatio-temporal variation of runoff coefficients on seasonal basis as well as for individual storms. Due to higher precipitation and topographic relief in the upland catchment of Silberhutte, the runoff coefficients were consistently higher and its peak was found in winter months due to lower evapotranspiration.

1. Introduction

Spatio-temporal variation of runoff generation processes in a catchment continues to be an active area of research. Stream network in a catchment is often viewed as an interconnected network/corridor for transfer of matter and solute from terrestrial landscape to the aquatic ecosystem. It is imperative to understand the runoff generation processes, i.e., source areas and pathways in a given catchment both for water quantity and quality purposes. For better management and implementation of flood protection measures it is essential to have a quantitative understanding of both base flow as well

---

* Corresponding author at: Geography Department, Durham University, Science Site, Durham, DH1 3LE, UK.
  E-mail addresses: sumit.sinha@durham.ac.uk, forsumit@gmail.com (S. Sinha).

as overland flow. With regard to the water quality point of view it is well known that different flow components transfer matter from terrestrial landscape to the aquatic ecosystem at different rates, (Lindstrom et al., 2010).

In order to characterize and quantify the aforementioned transfer rates it is necessary to understand the physics behind the runoff generation processes for a given catchment. Better understanding of the runoff generation processes is also potentially helpful in assessing the impact of land-use and climate change on the hydrological response of the catchment (Uhlenbrook et al., 2010; Neupane and Kumar, 2015). The complexity of the physics behind the runoff generation processes are partly attributed to partial decoupling of hydraulic response, as observed in the stream gauge data, from the actual flow paths through which the water is routed to the stream (Kirchner, 2003). The aforementioned partial decoupling alludes to the fact that in the vast majority of catchments, the hydraulic response is only partially driven by advective flow processes that are characterized by the translatory movement of water particles due to the elevation head. One of the major contributions to the stream flow is attributed to diffusive processes for example groundwater response and is majorly driven by the gradient of the pressure head.

Researchers have also reached a broad consensus on the three major runoff generation mechanisms which are: infiltration excess runoff, commonly known as Hortonian overland flow, saturation excess runoff, commonly known Dunne overland flow and subsurface flow. Discharge data observed at gauging stations are often the aggregate result of the aforementioned mechanisms. Combined experimental and numerical work has also revealed that relatively flat areas close to the stream are susceptible to quicker saturation even during small rainfall events and are able to rapidly deliver water to the stream network, resulting in a fast runoff response. However, soil water stored in the far stream hill slope zones may be released only during higher intensity rainfall events, when flow paths between hill slope and the riparian zone become connected. Some researchers have indicated storage as a critical element in the streamflow generation and have called for greater investigation of storage dynamics of the watershed (Spence, 2010). The dominant processes behind the runoff generation in a given catchment is highly variable in space and time and is attributed to the spatio-temporal variability of the precipitation, varying physiographic features of the catchment, infiltration, and antecedent conditions (Singh, 1997). As mentioned before the two main overland runoff generation mechanisms are infiltration excess, "Hortonian runoff" and saturation excess, "Dunne runoff". Depending on the antecedent soil moisture and storm intensity and duration, it is quite possible that soil may reach a state that precipitation exceeds infiltration capacity of the soil which leads to the infiltration excess or Hortonian runoff generation (Horton 1933). With regard to, "Dunne runoff", this usually occurs in the area with relatively shallow water table, the groundwater table due to the recharge from precipitation saturates the soil from below and reaches a point that any additional precipitation on such a saturated soil leads to runoff produced due to the saturation excess.

In order to examine, how the process of runoff generation varies and switches between the aforementioned major runoff-generating mechanisms spatially and temporally, a fully distributed or a semi-distributed model is typically needed. A successfully calibrated and validated hydrological model for a given catchment is in essence a virtual reflection of how a catchment functions (Tian et al., 2012). Different hydrological processes occurring at diverse spatial and temporal scales are typically represented by the different structural components of the model corresponding to physical realism of the model, (Hartmann et al., 2013). Multiple researchers have applied fully and semi-distributed models, some examples are (Reggiani et al., 2000; Vivoni et al., 2007; Yokoo et al., 2008; Li et al., 2012; Tian et al., 2012) among many others in order to investigate the physics behind the runoff generation processes. The aforementioned examples ranged from application of the model to hypothetical catchments, examining long term responses i.e. annual to seasonal and intra-annual and spatial variability of runoff generation mechanisms and event scale runoff coefficients.

The central premise of the work presented in this paper is to examine and understand the process of runoff generation in a mesoscale, Selke, catchment in central Germany with the help of the observed data as well as validated semi-distributed model. With the help of the rainfall-runoff data available on the daily time step, we examined the spatio-temporal variation of the runoff dynamics for the high flow events. The diagnostic analysis presented utilized runoff coefficient as the key signature to shed light on the spatial and temporal variability of runoff generation in the Selke catchment. The definition of runoff coefficient is presented in Section 2.3. Furthermore, we used the validated semi-distributed hydrological model, HYPE, (Lindstrom et al., 2010) to explore the space-time variability of runoff generating mechanisms in the Selke catchment. HYPE model has been extensively applied to catchments of varying sizes; some examples among many are (Arheimer et al., 2011; Arheimer and Lindström, 2013; Pechlivanidis and Arheimer, 2015). However, authors of this paper are not aware of any work that has used the HYPE model for examining the spatio-temporal variation of runoff generating mechanisms. It is also worth reiterating that data based analysis and model simulations presented in this work is based on daily time step as input data/observations were available on that time step. However, one should be cognizant about the fact that the analysis/simulations presented in this paper, if repeated, with finer temporal resolution might lead to somewhat different insights. The case in point is Vivoni et al. (2007) who showed the usefulness of high resolution input data for examining the runoff generation mechanism in a small catchment in Rio Salado basin in central New Mexico. More recently Anis and Rode (2015) investigated the hydrological dynamics and behaviour of the runoff components using high-resolution rainfall runoff modelling in Schafertal catchment in central Germany. They showed that the overland flow generated with 10-min simulation is larger than daily simulation and corresponds to better observed values.

The remainder of this paper is organized as follows. In Section 2, we describe the study area, key signature used for the analysis of the observed data and brief description of HYPE model and its setup for the Selke catchment. Section 3 presents
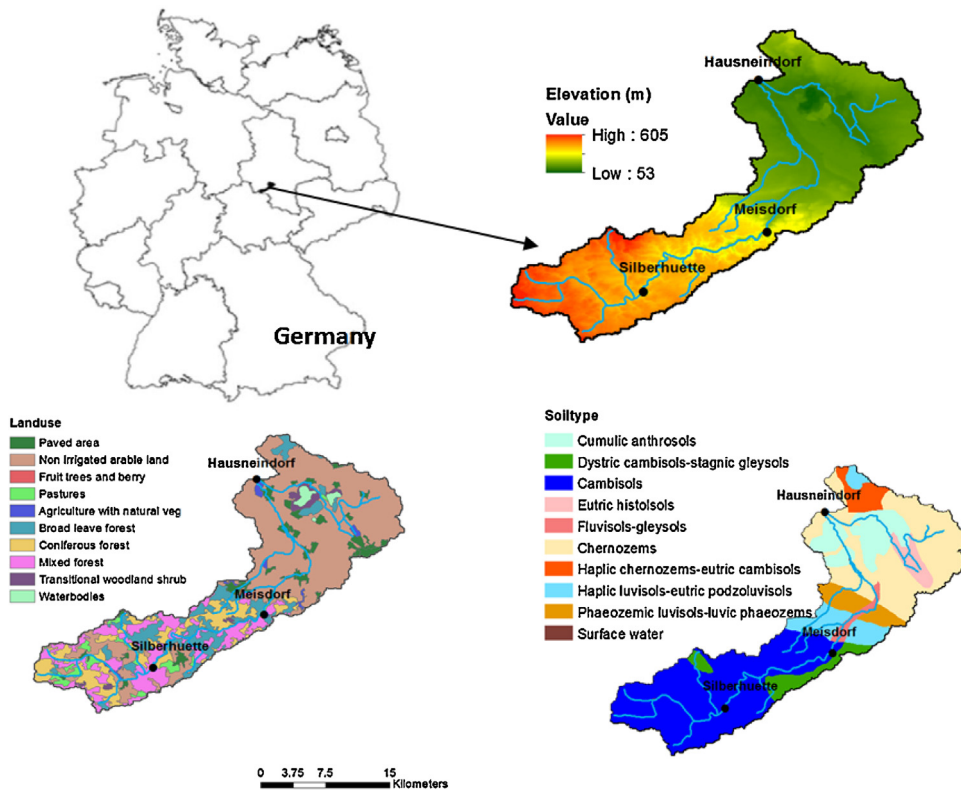
Fig. 1. Elevation, land-use and soil type of Selke catchment in central Germany.

the analysis of the results obtained from the processing of the observed data and application of the HYPE model. Finally, Section 4 presents the main conclusions along with the limitations and the future work.

2. Study area and methodology

In this section we describe the study area (catchment), available data, methodology used for the analysis of the observed data and finally description of the semi-distributed model (HYPE) used and its setup for the runoff modelling of the Selke catchment.

2.1. Study catchment

The catchment analysed in this research, Selke, is a tributary of the Bode River, which is one of four TERENO (TERrestrial ENvironmental Observatories) global change exploratories managed by the Helmholtz Association, Germany. The Selke catchment is a mesoscale, lower-mountain range catchment draining an area of 463 km² at the outlet gauging station at Hausneindorf (Fig. 1). The catchment is equipped with three gauging stations (Silberhuette, Meisdorf and Hausneindorf), where discharge and water quality parameters are measured. Daily discharge data are available for the whole Selke catchment at Hausneindorf (Fig. 1), covering an area of 463 km², as well as for the nested catchments of Meisdorf (184 km²) and Silberhutte (100 km²). The aforementioned streamflow data exhibits significant temporal variations characterized by high flow during winter (due to the combined effect of snowmelt and rainfall) and low flow with occasional high flows caused by storm events in summer. The Selke River originates in the Harz mountain range and discharges into the Bode River in the lowland areas. The elevation varies from 605 to 53 m (Fig. 1), from the headwater to the catchment outlet at Hausneindorf. Land use is dominated by forest (such as broad-leaved forest, coniferous forest and mixed forest) in the mountain areas and agriculture in the lowland areas (Fig. 1). The shares of agriculture and forest in the Selke catchment are 58% and 35%, respectively. The percentage of forest is greater in the upland area, whereas the low lying areas are dominated by agricultural land-use. Soil is dominated by cambisols in the mountain areas and chernozems in the lowland areas (Fig. 1). The underlying geology is characterized by schist and claystone in the upstream areas and tertiary sediments with loess in the downstream areas. The mean annual precipitation decreases from 792 mm in the Harz Mountain to 450 mm in the lowland areas, with an average of 660 mm for the whole Selke catchment. Amount of precipitation is greater in summer with a ratio of 1.35 between summer and winter values. The mean temperature is 9 °C, with an average monthly low of −1.8 °C in January and

high of 15.5 °C in July. There is an increase of temperature from the mountain areas to the downstream areas. There are 16 precipitation stations and 2 climate stations within/close to the Selke catchment and is maintained and operated by the German Weather Service (DWD). Precipitation stations are denser in the mountain areas compared with the lowland areas. Digital elevation model (DEM) at 90 m resolution and stream network data required for hydrological modelling is obtained from State Survey Office (Jiang et al., 2014). Soil type and land use data are available at 50 m and 25 m resolution respectively and were obtained from State Survey Office and Corine Land Cover 2006 dataset.

2.2. Estimation of potential evapotranspiration (PET)

Due to the limited availability of wide range meteorological data, at desired frequency, such as wind speed, relative humidity, solar radiation a temperature based method was adopted for estimation of Potential Evapotranspiration (PET) (Blaney and Criddle, 1950). Blaney-Criddle formulation has been used by several researchers in different locations (Benli et al., 2010; Razzaghi and Sepaskhah, 2010; Al-Faraj and Al-Dabbagh, 2015) successfully for estimation of PET and is presented in Eq. (1).

$$ET_o \left(mm/day \right) = P(0.46T_{mean} + 8) \tag{1}$$

In Eq. (1) ET_o denotes PET (mm/day), T_{mean} is the daily mean temperature (°C) and P is the mean daily percentage for annual day time hours for different latitudes. Daily values of PET, calculated from the above formulation and observed precipitation and discharge were averaged for monthly values. These monthly values were than averaged again for the number of years of data available i.e. 1993–2004.

2.3. Storm analysis

In order to examine the catchment behaviour and response during storm events and its partitioning of water into evaporation, runoff and recharge we adopted the diagnostic of runoff ratio/coefficient (McMillan et al., 2014) as mentioned in the introduction section. Runoff coefficient is computed by taking the ratio of total runoff depth and total precipitation for the time frame over which the runoff coefficient is desired. The aforementioned coefficient is indicative of the amount of rainfall that was transformed into runoff for the considered period. We computed the runoff coefficients for individual storm events (event runoff coefficient) as well as on seasonal basis (total runoff coefficient) with the help of data available for precipitation and discharge at the daily time step. The event runoff coefficient was computed by designating the start of the storm events when the precipitation was greater than 10 mm on a given day which was then followed by days of positive precipitation, the storm event ended when encountered two consecutive days of zero precipitation (McMillan et al., 2014). The computation of total runoff coefficient was done via two-step process. First the ratio of total runoff depth to total precipitation was computed for each season for a given year. These yearly values were than averaged over the total number of years, 1993–2004, for which the data were available.

2.4. Numerical model applied: Hydrological Prediction for the Environment (HYPE)

The semi-distributed model used for hydrological simulation in this research is Hydrologiska Byrans Vattenbalansavdelning (HBV), (Bergstorm, 1992; Lindstrom et al., 1997), inspired model Hydrological Predictions for the Environment (HYPE), (Lindstrom et al., 2010). The aforementioned model was developed by Swedish Meteorological and Hydrological Institute (SMHI) with main focus on integrating water quantity and quality processes at the landscape/catchment scale.

2.4.1. HYPE components

The HYPE model is capable of simulating hydrological processes like evapotranspiration, macropore flow, tile drain, surface runoff comprised of saturation excess and infiltration excess overland flow and soil moisture dynamics. The model is dynamical in nature forced by time-series of precipitation and air temperature, provided on a daily time step. The details of process implementation of HYPE model is given in (Lindstrom et al., 2010), brief description of major hydrological processes are provided here for the sake of continuity. As a first pre-processing step to the model application the catchment under consideration is first discretized into number of sub-basins as shown in Fig. 3. These sub-basins are connected through regional groundwater flow or/and rivers. Each sub-basin is than divided into multiple classes depending on the information derived from soil type and land-use cover, in HYPE jargon this is commonly known as SLC classes and is the smallest computational unit on which the model acts. It should be noted that these classes are not completely coupled to geographic locations rather defined as percentage of the sub-basin area. For example, depending on the soil type and land-use information, suppose fifty Soil-type Land-use Combination (SLC) classes may be proposed for a given catchment, a sub-basin, broader spatial unit into which the catchment was initially discretized, might only be covered with ten of those fifty SLC classes. Furthermore, different sub-basins might have different SLC classes present in them depending on the spatial heterogeneity of the soil type and the land use in the given catchment. Land and lake classes are treated differently by the model. The soil profile in each land class can be vertically divided from one to maximum of three layers of varying thickness. With regard to the model parameters, some are coupled to soil type; while others are land use dependent and then some are independent of soil type and land use and more general in nature and are constant for the entire domain. Hydrological simulations are performed on

daily time step; provision for one year warm-up period is made and is generally omitted from the evaluations. Model has been developed in FORTRAN and is modular in nature for further development and can run both on Windows as well Linux systems and is open source under GNU public license.

Below a certain threshold air temperature the precipitation falls as snow. The melting of the accumulated snow is modelled by degree-day method (Clyde, 1931; Collins, 1934) and uses the same threshold temperature as the snowfall process; the degree-day parameter is dependent on land-use type. The soil moisture for a given soil layer is inherently linked with three soil type dependent parameters representing: the fraction not available for evapotranspiration, the fraction available for evapotranspiration but not for runoff and the fraction available for runoff. The sum total of these three parameters indicates the maximum water content of the soil i.e. total porosity of the soil. The first two fractions correspond to the concept of wilting point and field capacity, measurable quantity but the model refrains from using these terms as there is no guarantee that the measured values can be directly used while applying the model. Evapotranspiration is allowed only from top two soil layers; hence the depth of second soil layer can be viewed as the rooting depth. The rate of actual evapotranspiration is computed as a function of difference between potential evapotranspiration and a soil-type dependent parameter that is indicative of maximum water content not available for evapotranspiration. As the model was developed by SMHI and initially applied to Swedish catchments where the depth to the groundwater table is quite shallow, typically in the order of some meters, no separate compartment for the groundwater flow is made in the model. The soil water content in the individual soil layer determines the height of the relatively shallow groundwater table. A fraction of rainfall and snowmelt taken as infiltration for the top soil layer is diverted as flow through the macropore and infiltration excess overland flow (Hortran overland flow) depending on threshold values which is a soil type dependent parameter. If the soil moisture in the uppermost soil layer exceeds maximum allowable water content the saturated overland flow occurs (Dunne overland flow). Excess soil water can drain from any layer (subsurface flow) if the soil moisture in that layer exceeds the threshold for runoff, which is again a soil-type dependent parameter. The discharge from soil, tile drains and surface runoff is directed towards the local stream. For routing the flow through the catchment, the stream network is broken into two surface water compartments which are linked in series. These compartments are local stream compartment which corresponds to the runoff generated in a sub-basin and a main stream compartment which corresponds to the sum of the runoff generated from the upstream basins (Fig. 3). In both of these compartments the flow is routed through postponing the peak, through simple time lag mechanism, and dampening the flow depending on the river length and flood wave velocity. The river length in the sub-basin is approximated by the square root of the sub-basin area if not given as an input. In addition to the delay, the flow peak can also be attenuated; this damping is implemented with the help of a recession coefficient which is dependent on the mean slope of the sub-basin.

2.4.2. HYPE setup for the Selke catchment

Selke catchment was delineated into 29 sub-basins (Fig. 4) based on the topography for the application of the HYPE model (Jiang et al., 2014). Furthermore, depending on soil type information and land uses cover, 117 different combinations of soil type and land use (SLC) classes were defined. Each sub-basin was then characterized by combination of fraction-percentage of SLCs as shown in Fig. 5. HYPE is a semi-distributed model because SLCs within each sub-basin are lumped. Depending on the heterogeneity of the soil type and land use and the area of the sub-basin; number of SLCs within different sub-basins varied from 1 in the sub-basin no. 13–47 in the sub-basin no. 19 (Fig. 5). The average slope, area and number of active SLCs for all the 29 delineated sub-basins is shown in Fig. 5. As the sub-basins are obtained by topographic delineation of the catchment, larger sub-basins tend to be characterized with greater number of active SLCs e.g., sub-basin no. 25 with an area of $47.98 \, km^2$ is defined with 45 active SLCs whereas sub-basin no. 13 with an area of $0.05 \, km^2$ is defined with just 1 active SLC. The outlet of the upland catchment of Silberhutte draining an area of $100 \, km^2$ is located in the sub-basin 28. Meisdorf drains an area of $184 \, km^2$ and its outlet is located in sub-basin 29 (Fig. 4a), finally the outlet of the whole Selke catchment draining an area of $463 \, km^2$, is located in the sub-basin 2 as shown in Fig. 4a. The drainage network on the sub-basin level as used for flow routing by the HYPE model is shown in Fig. 4b. The runoff and its components obtained at the outlet of any sub-basin is the sum total of the runoff produced by that sub-basin as well as the runoff routed through the sub-basin drainage network from the upstream area (Fig. 4b).

It is worth reiterating that the objective of this research is not apply and calibrate the HYPE model for the Selke catchment, rather use the validated model (Jiang et al., 2014) to gain insights into the space-time variability of runoff generation mechanisms as observed in the considered catchment. In order to examine the spatial and temporal variation of runoff generation mechanisms in the Selke catchment, HYPE code was modified and some additional simulations were conducted using the validated model for generating outputs relevant to this research. As mentioned before the runoff generated at the sub-basin level is computed by the model as the sum of the runoff generated by the contributing SLCs, weighted by their area-percentage-fraction in the sub-basin, which in turn is comprised of runoff generated from different soil layers, macropore flow, tile drain flow, saturation excess overland flow and infiltration excess overland flow. The total runoff generated by each sub-basin is than routed through the catchment according to the algorithm explained in Section 2.4.1. In order to examine the spatio-temporal variation of Dunne and Hortonian overland flow, the HYPE model was modified to store these components of the runoff separately from each sub-basin and was than routed through the catchment according to the same routing algorithm as explained before. As HYPE is a semi-distributed model fluxes are stored at the outlet of the discretized sub-basins hence it was possible to compute relevant contribution from different flow components as the runoff was routed through the catchment. With regard to the further processing of the simulation based data, the model based total seasonal

Table 1
Total runoff-coefficient based on average value over different seasons for the three nested catchments.

Season\Catchment	Hausneindorf	Meisdorf	Silberhutte
Winter	0.34	0.66	0.72
Spring	0.30	0.65	0.75
Summer	0.06	0.14	0.15
Autumn	0.12	0.24	0.29

runoff coefficients, for each sub-basin, was calculated by taking the ratio of the total simulated runoff for a given season for the entire stretch of the simulated period and the total precipitation received by the sub-basin, given as an input to the model, for the season under consideration during the simulation period. Precipitation for each sub-basin, specified as an input on daily timestep, was interpolated from the nearest meteorological station. The ratio computed in a similar fashion with Horton and Dunne overland runoff gave Horton and Dunne runoff coefficients on seasonal basis.

As mentioned before while applying the HYPE model each sub-basin was discretized into different numbers of active SLC units which in turn was characterized by varying number of soil layers, maximum three, having different thickness. The soil saturation on a given day for an active SLC, smallest computational unit on which the model acts, was calculated as the ratio of soil moisture to the total porosity for each soil layer which is then averaged over the number of soil layers present in that SLC weighted by the thickness of the individual layers. Finally, within the sub-basin, spatial averaging weighted by the area percentage of contributing SLCs is done to find the single representative daily value of the soil saturation for the sub-basin under consideration. The arithmetic average of these daily values taken over a given season gives us the degree of the seasonal-averaged soil saturation.

3. Results and discussion

3.1. Variation of precipitation, temperature and potential evapotranspiration

The maximum precipitation, for the analysed time frame, between 01/01/1994 and 01/01/2004, was observed on April 12, 1994, and was observed to be approximately 80 mm/day for Silberhutte and Meisdorf (Fig. 2) and nearly 60 mm for Hausneindorf. The maximum runoff was recorded a day after the intense storm event for the upland area of Silberhutte and Meisdorf and was around 47 m³/s and 38 m³/s respectively. At the outlet of the Selke catchment, Hausneindorf, the peak discharge was recorded two days after the aforementioned intense storm event and was around 54 m³/s (Fig. 2). Daily PET values, calculated from Eq. (1), observed precipitation and discharge values were averaged over individual months. These monthly values were than averaged again for the number of years of data available, 1994–2004, and is presented in Fig. 6 for all the three catchments i.e. Silberhutte, Meisdorf and Hausneindorf. PET estimates for all the three catchments shows maximum value during the summer months, the peak is observed at an average of 6 mm/day in the month of June, this is expected because of the linear relation between PET and the average temperature as shown in Eq. (1). However, in the upland catchments there is approximately 12% decrease in this peak and maximum PET for Silberhutte is observed around 5.2 mm/day again in the month of June. The temporal variation of runoff exhibits opposite trend to PET with lowest discharge occurring in summer months and an increasing trend in winter and early spring (Fig. 2). Average monthly precipitation estimated on daily basis doesn't show a distinctly different values between months, hence lower discharge during summer months can be potentially attributed to the higher PET values in the summer months. Although PET estimates are based only on mean temperature values, Eq. (1), and doesn't take in account other relevant meteorological data such as wind speed, relative humidity and solar radiation it still gives a first-order approximation of temporal trend of PET in the catchment.

3.2. High-flow events

The seasonal variations in the total runoff coefficient for the three gauging stations are presented in Table 1. We consistently observed higher total runoff coefficients in winter and spring which can be potentially attributed to the combined effect of snowmelt and winter rain. The minimum total runoff coefficient across all the catchments was observed during summer and is lowest for Hausneindorf (Table 1). This can be potentially explained by the fact that the total runoff coefficient is controlled by the water which is not consumed by the evaporation and ground water fluxes (McMillan et al., 2014), in the summer months due to the higher PET values significant portion of water is lost to evaporative fluxes consequently total runoff coefficient is at its lowest. With regard to the spatial variation of the runoff coefficient, It is worth highlighting that the total runoff coefficient is generally higher in the sub-nested upland catchment of Silberhutte (Table 1) which may be explained by higher topographic relief combined with more frequent and longer precipitation events at higher elevation.

In Fig. 7, we present three-dimensional plots characterizing the storm events. The month of occurrence of the storm events is presented on the x-axis, average precipitation in mm/day for the storm events on the y-axis and event-runoff coefficient on the z axis. The event runoff coefficient varies between 0 and 1, with 0 indicating no runoff generated and when all the precipitation turns into runoff, the value of the runoff coefficient is 1. Furthermore, the storm events are depicted by spheres of varying size and are colour according to the duration of the storm events. Longer storm events are depicted by spheres of
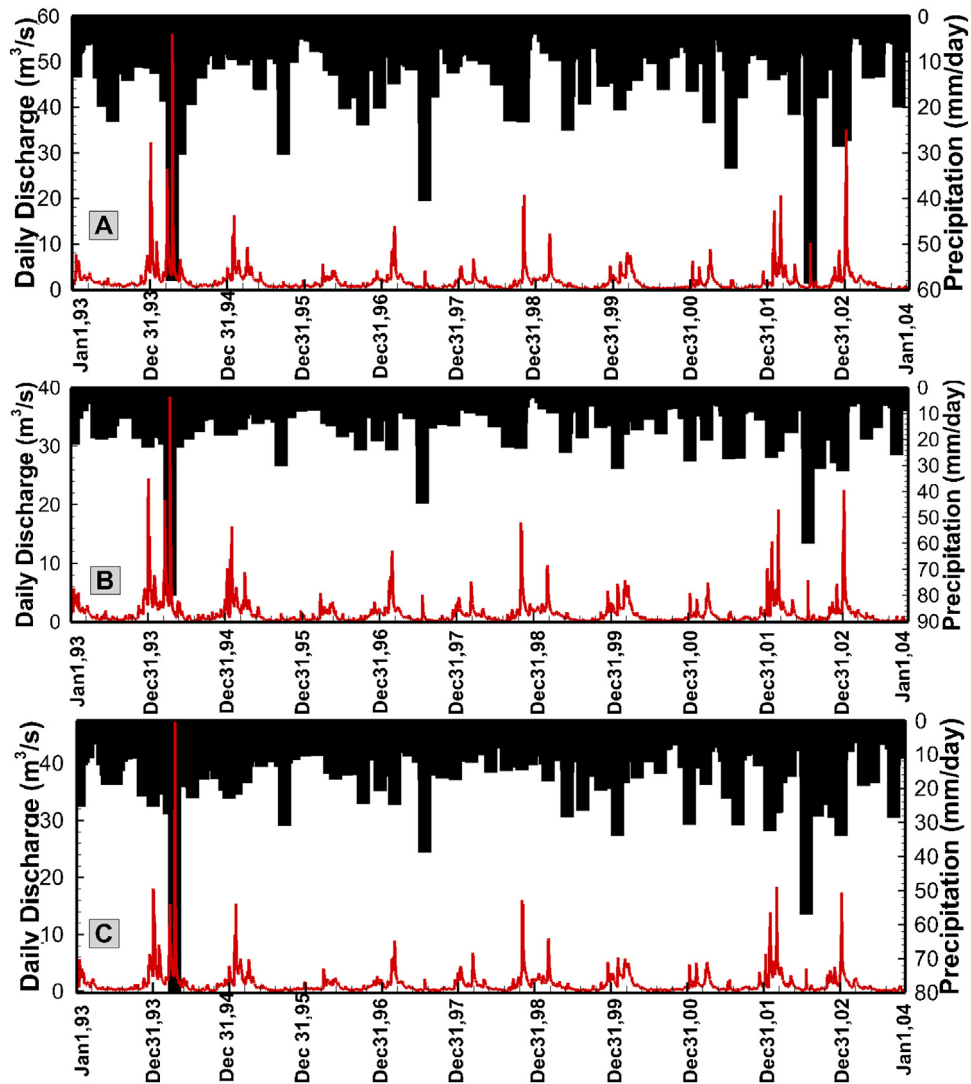
Fig. 2. Daily discharge and precipitation for 1993-2004 at (A) Hausneindorf (B) Meisdorf and (C) Silberhutte.

bigger size and colours tending towards red, shorter storm events are shown by the spheres of smaller size and are coloured in blue. The duration of the identified storm events, according to the aforementioned criteria (Section 2.3), was found to be maximum thirty days, however, realistically storm events in the Selke catchment does not persist beyond five days, hence the storm events with duration between one and five days are shown (Fig. 7). It should be noted that the longer storm events tends to have lower average precipitation during the event as shown in Fig. 7. Consistent with the seasonal pattern of total runoff coefficient, higher event runoff coefficient is observed for the sub-nested and upland catchment of Silberhutte (red sphere Fig. 7a) and occurs during the winter months. This could be explained by the combined effect of snow melting and greater slopes in the upland area. A general decrease in the duration of storm and values of the event runoff coefficient from the upland catchment of Silberhutte to the lower areas of Meisdorf and Hausneindorf was observed. This general decrease in the event runoff coefficient for the bigger catchments of Meisdorf and Hausneindorf, can be potentially and partially attributed to the vertical groundwater flux as larger areas of watershed are brought under consideration (McMillan et al., 2014). Also in the low lying areas due to the decrease in the topographic slope the runoff coefficient is expected to decrease as shown (Fig. 7).

3.3. Hype modelling results

The comparison between the simulated and the observed discharge at all the three gauging stations in the Selke catchment is shown in Fig. 8. The simulation was conducted for a ten-year period between Jan 1, 1994 to Jan 1, 2004 with the year 1993 used as the warm-up year. As shown in Fig. 8 the model is able to capture the temporal dynamics of discharge at the
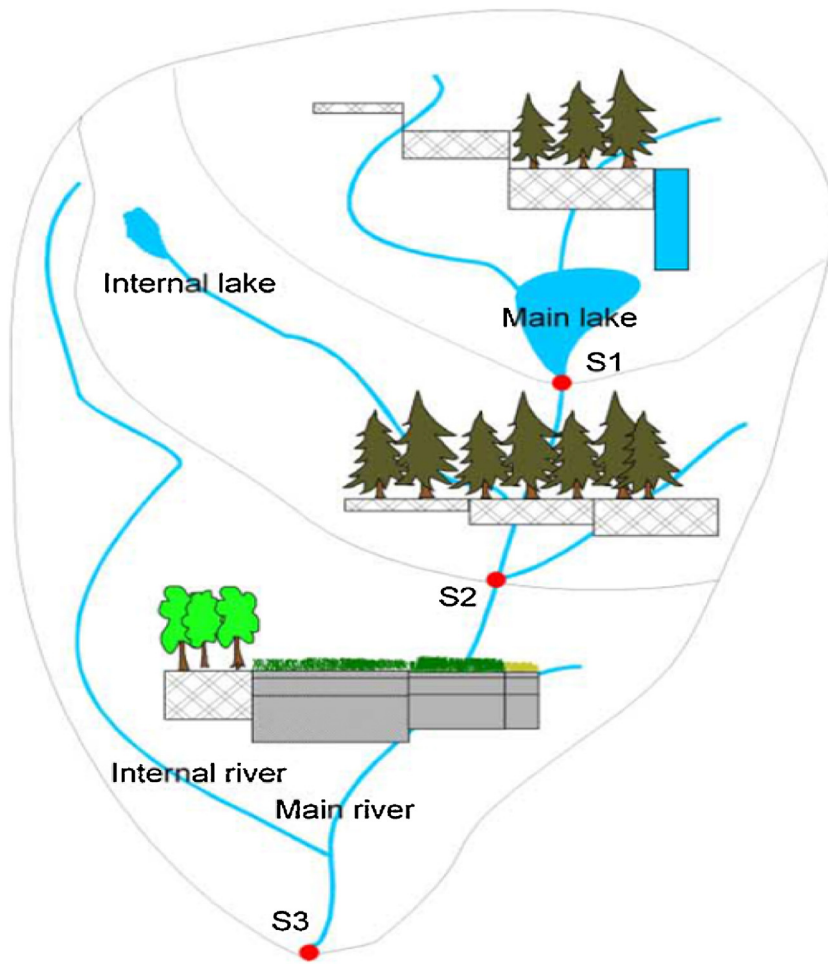
Fig. 3. Schematic depicting the division and connections between multiple sub-basins denoted by S1, S2 and S3 in a catchment (Lindstrom et al., 2010).
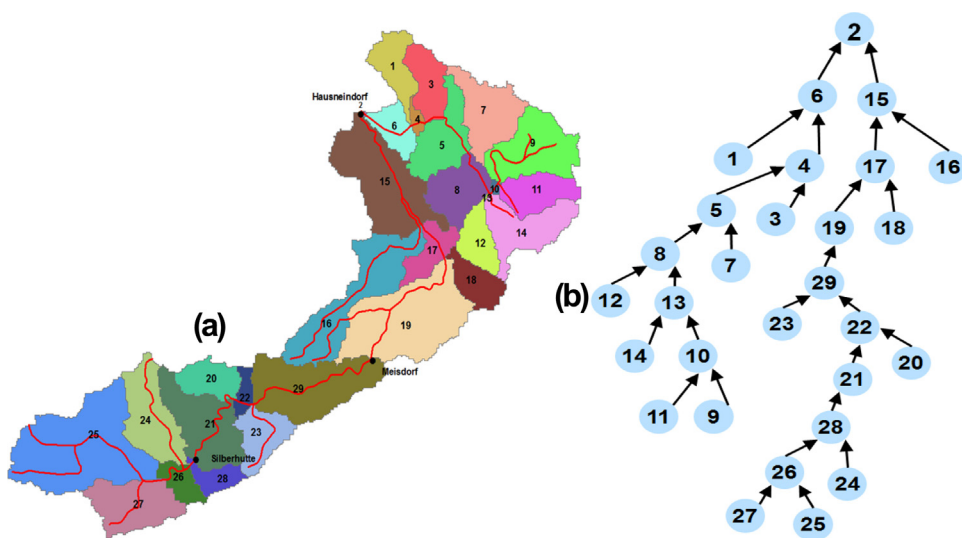

Fig. 4. (a) 29 sub-basins Selke catchment was discretized for HYPE application (b) drainage network of the discretized sub-basin, the final outlet is at Hausneindorf denoted by sub-basin 2.
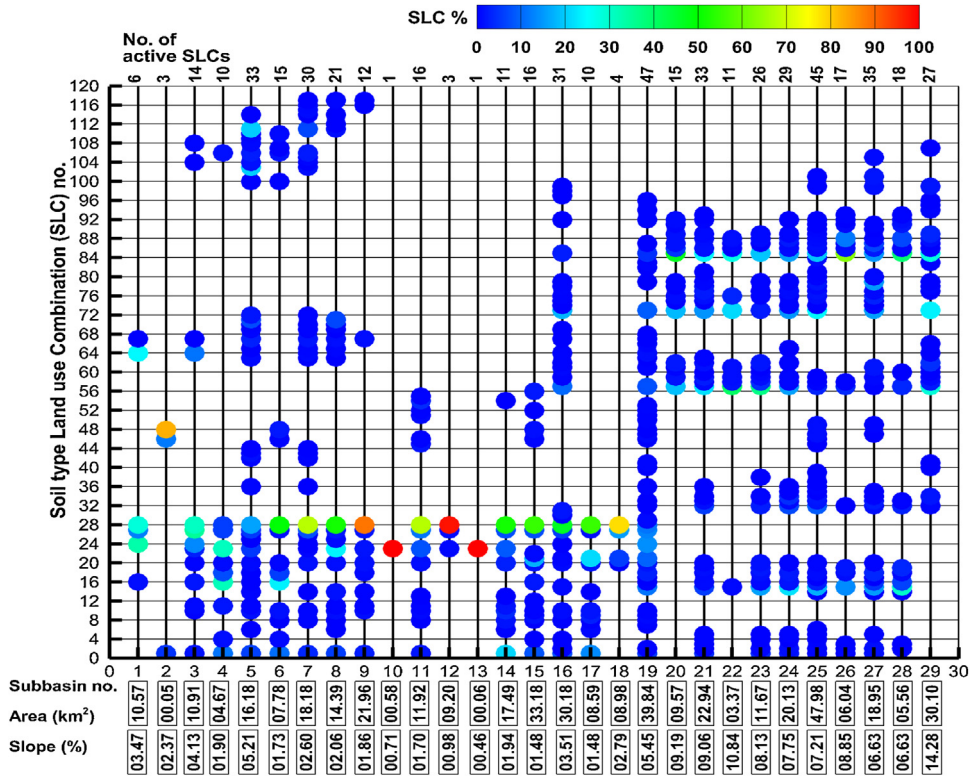
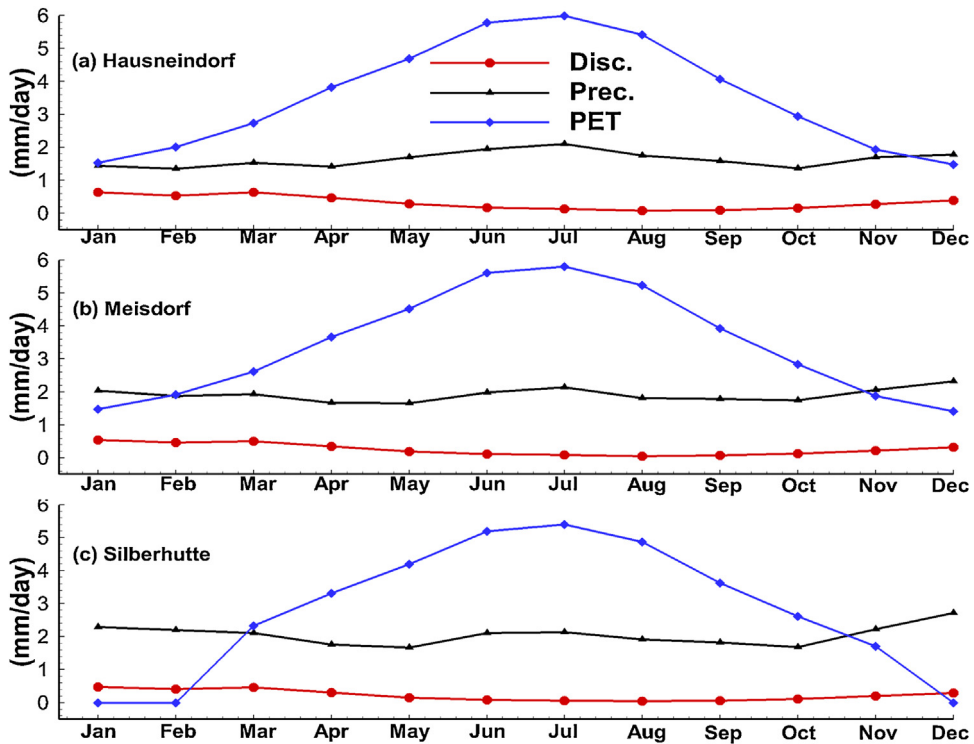**Fig. 5.** Total number and percentages of SLCs for each discretized sub-basin along with sub-basin's area and average slope.

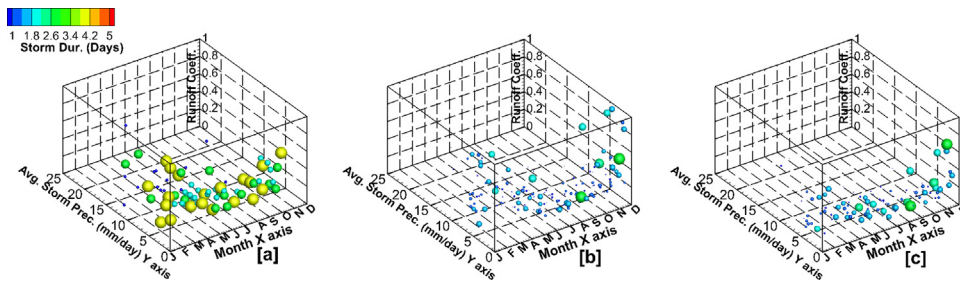**Fig. 6.** Average monthly discharge, precipitation and PET in (mm/day) for the three catchments.

Fig. 7. Storm events plotted according to month of occurrence, average precipitation in mm/day during the event, and runoff coefficient during the storm. Events are denoted with spheres of size and colour dependent on the duration of storm in days [a] Silberhutte, [b] Meisdorf and [c] is Hausneindorf.
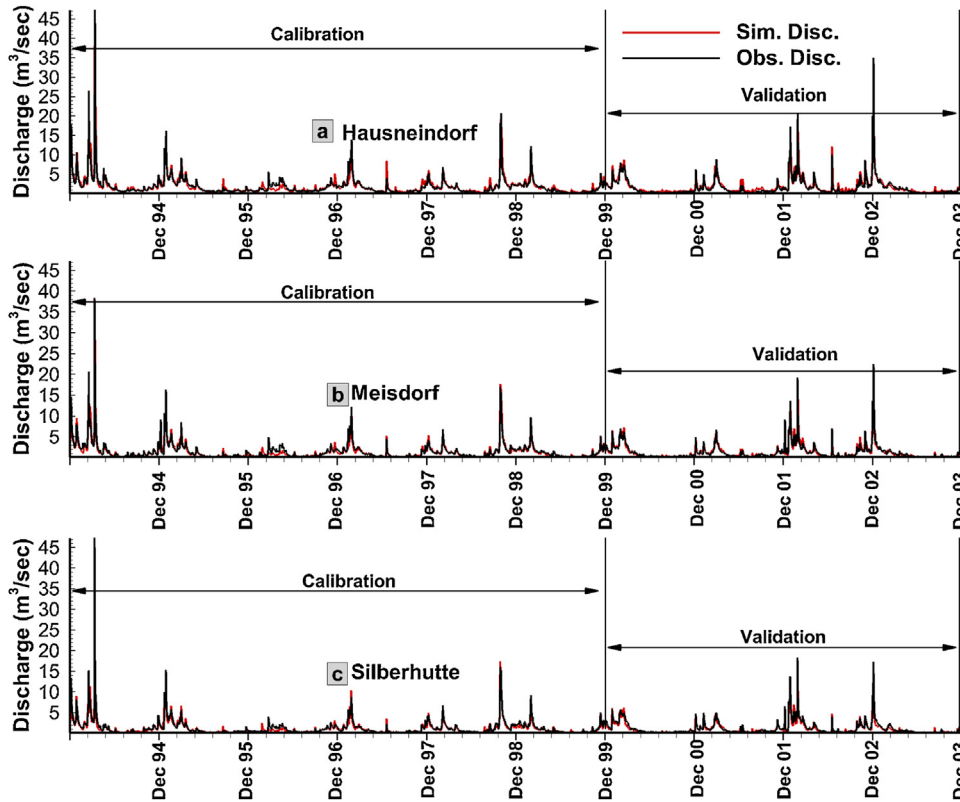

Fig. 8. Comparaison between simulated and observed discharge at gauging stations (a) Hausneindorf (b) Meisdorf (c) Silberhutte with validated model.

outlet (Hausneindorf gauging station) as well as at inlet stations (Meisdorf and Silberhutte) in a satisfactory manner. Model calibration was done with the help of split-sampling approach, with 1994–1999 used for calibration and 2000–2004 used for validation. Parameter estimates resulting in the best values for the formulated objective functions were obtained with the help of PEST (Doherty, 2005). For details on the parameter sensitivity and estimation for the HYPE model as applied to the Selke catchment, please refer (Jiang et al., 2014). The statistical criteria used for model calibration and parameter estimation are the coefficient of determination (R^2), Nash-Suttcliffe efficiency (NSE), percentage bias (PBIAS) and root mean squared error (RMSE). Definition and detailed description of these criteria are given in numerous studies (e.g. Gupta et al., 1999; Moriasi et al., 2007; Nash and Suttcliffe, 1970). The values of the different objective functions obtained during calibration and validation is presented in Table 2. It must be reiterated that the model calibration and validation was done by Jiang et al. (2014) and presented here for the sake of continuity.

The comparative contribution from Dunne overland flow, Hortonian runoff and sub-surface flow as obtained from the modified HYPE model from the simulations conducted for the aforementioned duration with the validated parameter sets at the three gauging stations is presented in Fig. 9. It is quite evident that the sub-surface flow is the primary runoff generating mechanism in the Selke catchment. It is also worth noting that Dunne overland flow exceeds the sub-surface flow component only during intense storm events (Fig. 9). Hortonian runoff generation mechanism has the minimum contribution to the total runoff and is expected for non-arid environment and is consistent with Dunne's conceptualisation of the spatial variation in

Table 2

Model evaluation statistics for discharge at the gauging stations Silberhutte, Meisdorf and Hausneindorf during calibration (1994–1999) and validation (1999–2004) periods, adopted from Jiang et al., 2014.

Variable	Criterion	Calibration			Validation		
		Silberhutte	Meisdorf	Hausneindorf	Silberhutte	Meisdorf	Hausneindorf
Discharge	R^2	0.89	0.88	0.86	0.92	0.90	0.88
	NSE	0.88	0.88	0.86	0.91	0.90	0.86
	PBIAS	−4.9	−3.8	2.6	−10.3	−0.7	14.3
	RSR	0.34	0.35	0.37	0.31	0.32	0.37
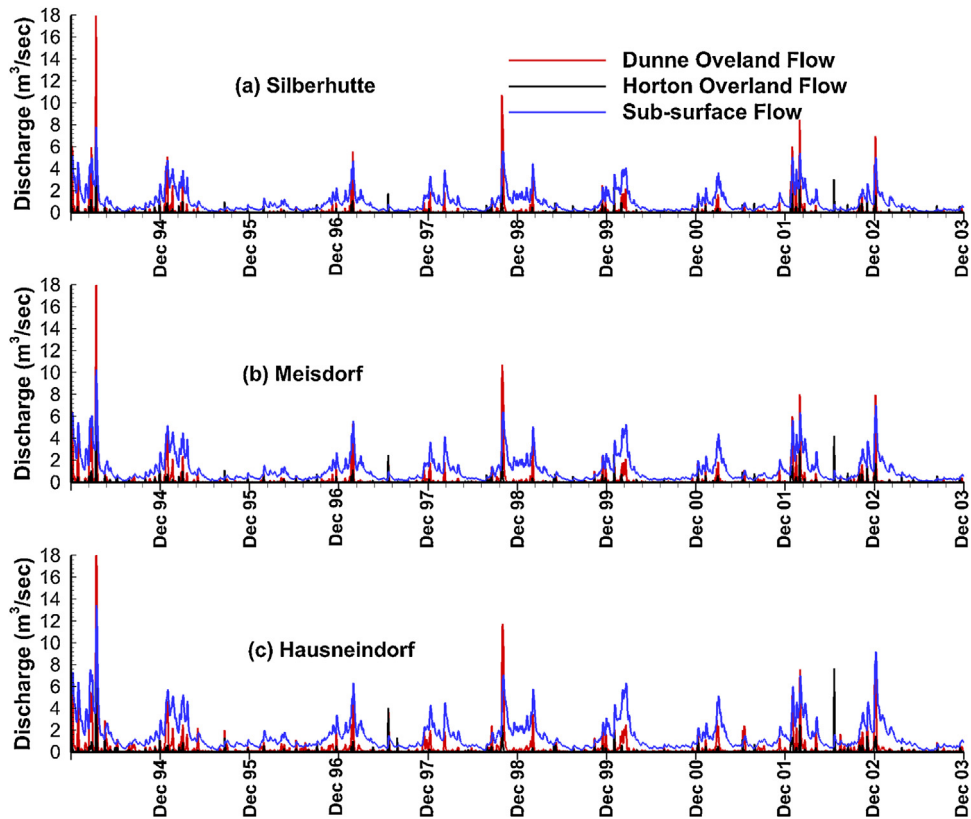
Fig. 9. Dunne overland flow, Horton overland flow and sub-surface flow at three gauging stations (a) Silberhutte, (b) Meisdorf and (c) Hausneindorf as obtained by the model simulations.

runoff generation mechanisms under different combinations of climate soil and topography (Dunne, 1978; Freeze, 1980). Furthermore, evident on a closer inspection, the peak of the Dunne overland flow, during storm events, exhibit a diminishing trend between the upland area of Silberhutte and low lying areas of Hausneindorf, this can be attributed to the difference in the topographic relief between the upland and the low-lying areas.

The spatial variation of the total runoff coefficient (Fig. 10) as obtained by the simulation consistently exhibited higher values in the upland area of Silberhutte and is at maximum during the winter months. This can be explained by the higher slopes (Fig. 5) and greater precipitation (Fig. 12) received by the sub-basins draining the upland catchment of Sliberhutte. It is quite evident that the seasonal variability in the runoff coefficient is primarily driven by the climatic forcing, whereas the spatial variabilities are controlled by the landscape properties. Similar conclusion has also been presented by Li et al. (2012) in a study of similar nature albeit using a different semi-distributed model. As the runoff is inherently linked with soil moisture dynamics (Western et al., 1998; Trom-van Meerveld and McDonnell, 2005; Latron and Gallart, 2008; James and Roulet, 2009; Zehe et al., 2010; Penna et al., 2011) a distinct positive correlation between the total runoff coefficients (Fig. 10) and the soil moisture saturation (Fig. 11) is observed. Positive correlation between soil moisture and runoff coefficient has also been observed by Woods et al. (2001) in an experimental watershed. In order to further explore the relation between runoff and soil moisture we plotted the comparative trend between averaged daily simulated runoff (mm) and degree of soil moisture saturation as obtained by the model on seasonal basis for the entire catchment, presented in Fig. 12. Both the daily runoff and the degree of soil moisture saturation were averaged across the entire simulation period for each day, these averaged values were then combined on seasonal basis and correlation between runoff and saturation was examined. The
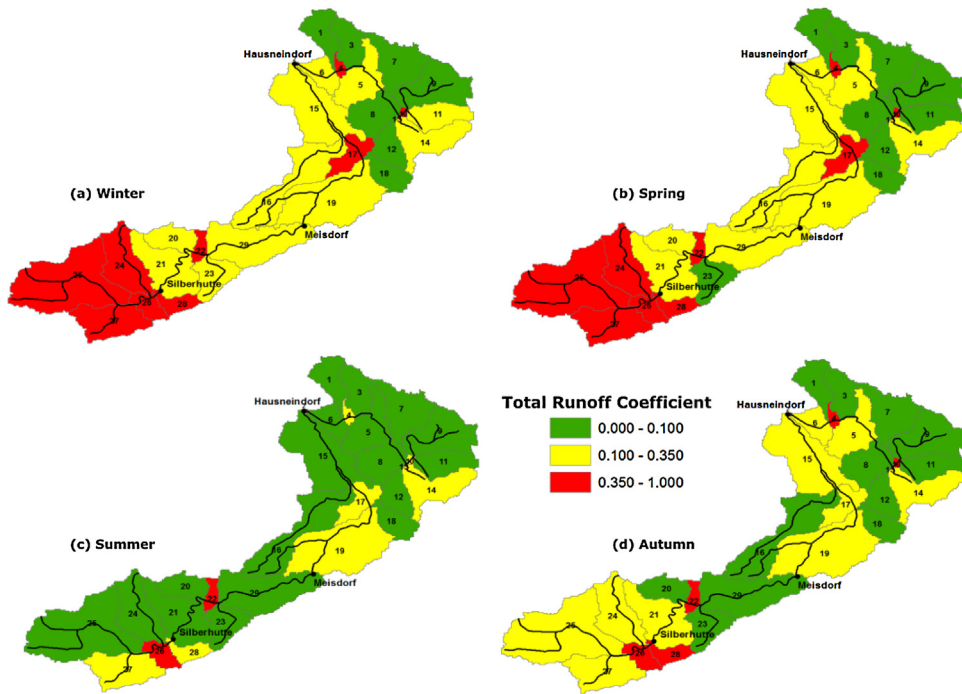
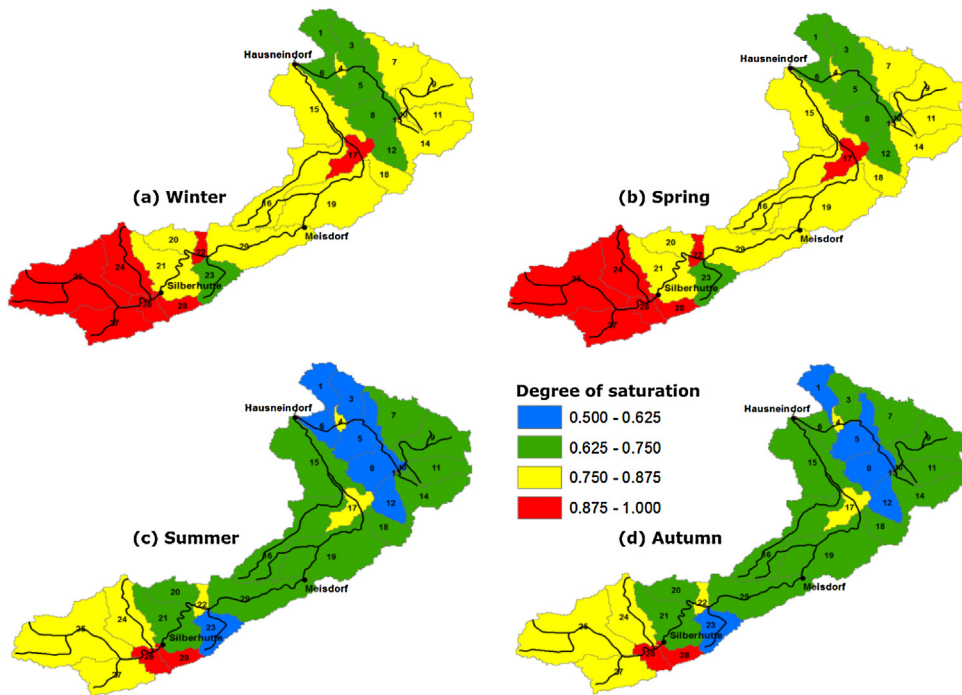**Fig. 10.** Spatial variation of total runoff coefficient with season.

Fig. 11. Spatial variation of seasonal-averaged soil saturation.

strongest positive correlation between the simulated daily runoff and degree of soil saturation was found for the month of spring followed by winter which can be potentially attributed to snowmelt and low evapotranspiration in winter and spring leading to persistent high soil saturation resulting in higher runoff. Both the degree of soil saturation and the total runoff as obtained by the model simulation (Fig. 12) are lesser for the summer and autumn months potentially due to the higher evaporative fluxes.
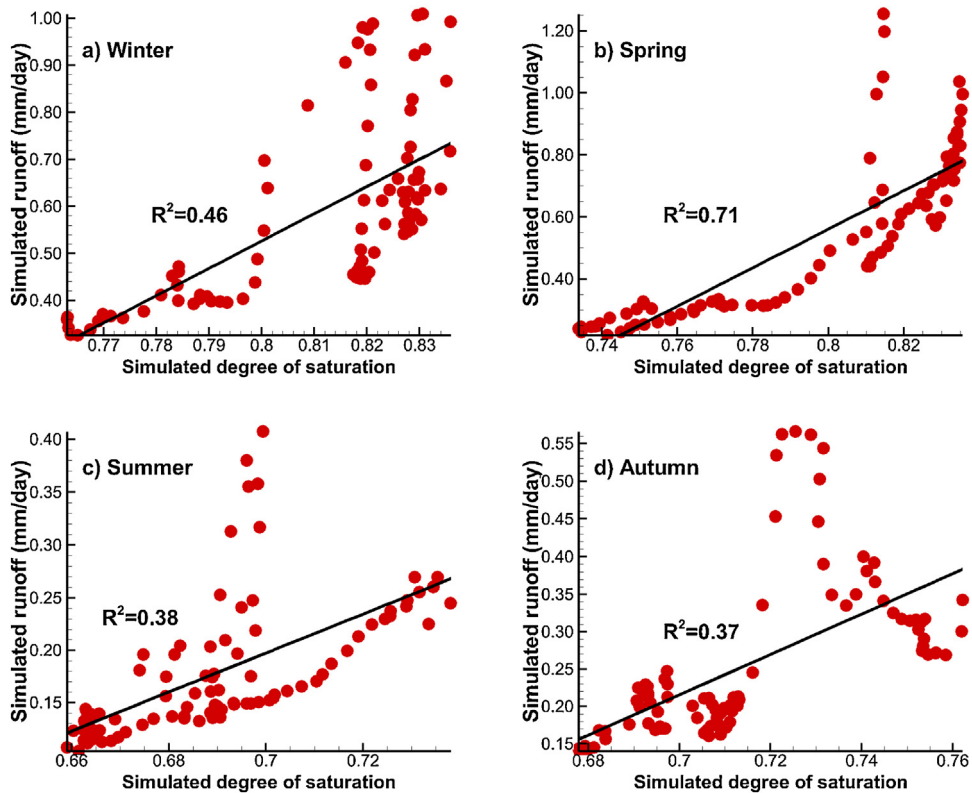
Fig. 12. Comparative plots between simulated runoff and degree of saturation on daily time step, presented on seasonal basis.

The sub-basins drained by Silberhutte and Meisdorf are marked by numbers 20 and above (Fig. 4) and received the net precipitation of more than 1400 mm, summed for various seasons for the entire simulated period (Fig. 13). The average slope of the discretized sub-basins, used in the HYPE model, were consistently higher in the upland area with slope-values in excess of 8% and reaching a maximum value of 14% in the upland area (Fig. 5). This can potentially explain the higher total runoff coefficient obtained by the model in the upland area (Fig. 10). Additionally, it should also be reiterated that one of the crucial characteristic properties for the runoff generation is the soil field capacity, however, HYPE model uses this as a calibrating parameter and refrains from the usage of this term as the calibrated value might be significantly different from what is measured. It is interesting to note that although the highest net precipitation is observed during the summer months in the upland area the total runoff coefficient as obtained by the model simulation is highest in the winter months, which can be explained by the higher soil saturation during the winter months (Fig. 11) combined with the snow melting. Due to the higher PET values during summer months (Fig. 6), despite marginally higher precipitation the soil saturation stays comparatively lower resulting in lower runoff coefficients as obtained by the model for the upland catchment of Silberhutte and Meisdorf.

The spatial variation for seasonal-averaged soil saturation as obtained by model simulations for various sub-basins and total precipitation obtained by the interpolation of observed data for each sub-basin, which is used as input data for the HYPE model, is presented in Figs. 11 and 13 respectively. Both precipitation and soil saturation exhibit a diminishing trend between upland and low lying areas which is of consequence for the total runoff coefficient (Fig. 10).

Once again, spatially and temporally similar trends as observed for the total runoff coefficient and the soil saturation are observed for the model-based Dunne runoff coefficient also (Fig. 14). The highest value of the Dunne runoff coefficient is observed in the upland catchment of Silberhutte and occurs in the winter months, the aforementioned coefficient diminishes during spring and reaches its minima in summer and reverts towards an increasing trend with onset of autumn (Fig. 14).

With regard to the model based calculation of various flow components, it is worth reiterating that like another commonly used semi-distributed model SWAT (Arnold et al., 1998), in HYPE also the smallest spatial unit of the domain obtained by topographic delineation is the sub-basin which is physically connected and contiguous to one another. However, the smallest computational units, on which the kernel of the hydrological model acts, are number of SLC classes within the sub-basin. Each sub-basin is comprised of varying percentages of different SLC units (Fig. 5) and they are principally non-geo-located, non-contiguous conceptual units based on homogenous land use and soil type. The lumping of sub-basins into SLCs speeds up the computational process, however, no provision is made for interaction between the SLCs units inside the sub-basin.
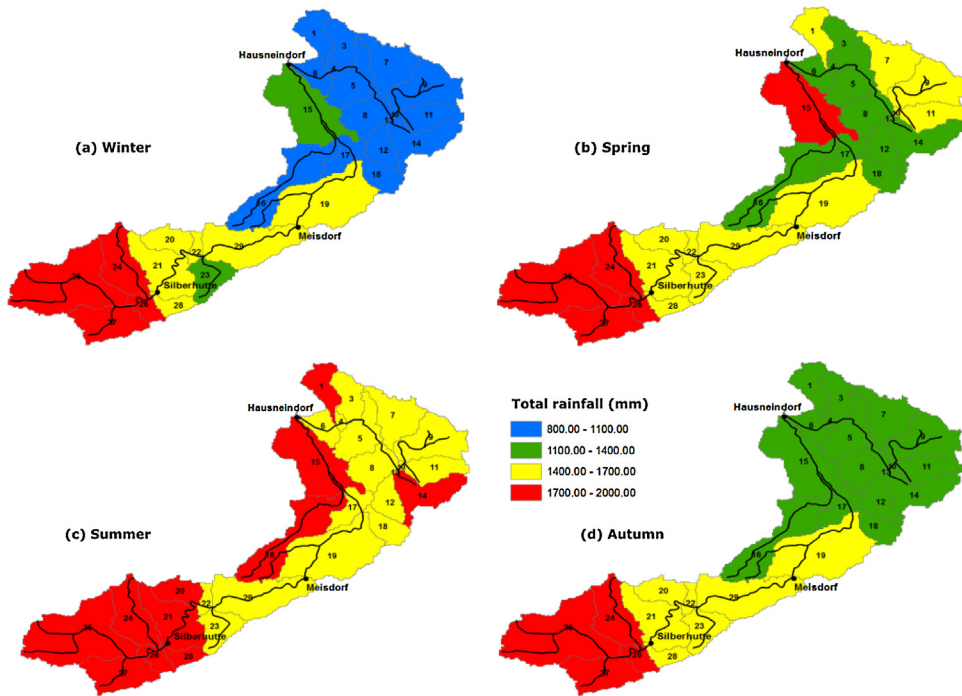
Fig. 13. Spatial variation of net rainfall (mm) for different seasons.
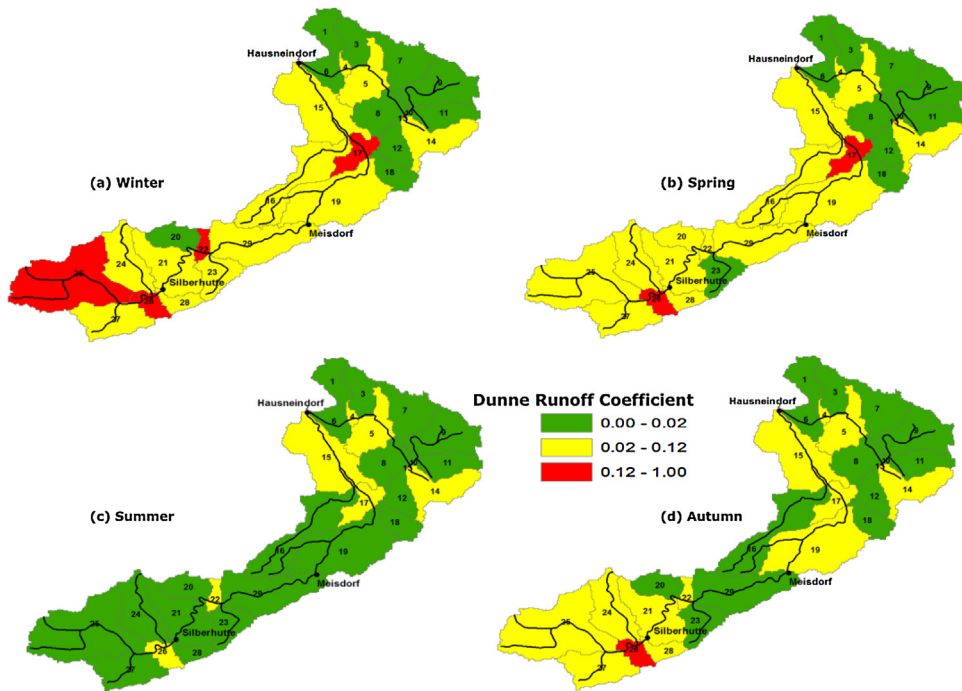

Fig. 14. Spatial variation of the Dunne runoff coefficient according to different seasons.

This approach is also followed by widely used SWAT model and has both limitations and advantages (Garen and Moore, 2005; Walter and Shaw, 2005).

Finally, to conclude the model based spatio-temporal analysis of the runoff generation processes, we examined the infiltration excess runoff, Hortonian overland flow, generated by the various sub-basins averaged on seasonal basis Fig.15. As shown in Fig.15 the magnitude of Hortonian overland runoff coefficient, as obtained by the model simulations, is an order

of magnitude lower in comparison to the model-based Dunne and Total runoff coefficient, which implies that both amount and frequency of the Hortonian overland runoff is drastically less than the runoff generated by other major mechanisms (Fig. 9). Furthermore, the spatial trend observed in regard with the model-based Hortonian runoff coefficient is not identical to the Total (Fig. 10) and Dunne runoff coefficient (Fig. 14) as obtained by the model. During the winter months high Hortonian runoff coefficients are only observed for sub-basins 24, 25, 26 and 27 located in highest elevation zone in the upland area(Fig. 4) which might again be attributed to higher precipitation in these areas. In contrast to the temporal trend observed for the model-based Total and Dunne runoff coefficient, the Hortonian runoff coefficient as obtained by the simulation is not at its minimum during summer months. Finally, it must be mentioned and as postulated by Dunne and Leopold (1978) Hortonian overland flow generally dominates the outlet hydrograph in arid to sub-humid climate combined with thin vegetation and areas majorly influenced by anthropogenic pressures unlike the Selke catchment which has been analysed in this research.

4. Conclusion

This paper has investigated the patterns of intra-annual variability of runoff generation mechanisms in the Selke river basin through systematic analysis of rainfall-runoff data available on the daily time step as well as application of a conceptual semi-distributed hydrological model HYPE. The key signature used for the analysis of the observed rainfall-runoff data, available on daily time step, was runoff coefficient which was consistently higher in the winter months (Table 2) which is potentially attributed to the lower PET estimates in winter. It is also worth highlighting that in the winter months, especially in December and January the ratio of precipitation to PET, Fig. 6, was distinctly greater than 1 with highest values observed in Silberhutte which implies higher humidity and is of consequence for the runoff coefficients. Event based runoff coefficients showed similar temporal trends and was found to be at its maximum in the winter months (Fig. 7). With regard to spatial variation of the runoff coefficient, the upland catchment consistently had higher values (Fig. 7a) which is attributed to the greater topographic relief in the high elevation areas.

With regard to the sptio-temporal variation of the major runoff generation mechanisms, the HYPE model was used for the first time, to the best of the knowledge of the authors of the current work, for examining and isolating the primary runoff generation processes in Selke and the nested catchments. The model based simulations showed that the major portion of discharge observed at the gauging stations for all the three catchments (nested) under consideration originated from sub-surface runoff (Fig. 9). Furthermore, Dunne overland flow, as obtained by the model simulations, exceeded the contribution from model-based sub-surface runoff very rarely. Model-based runoff coefficients were consistently higher in the upland area, especially Total and Dunne runoff coefficient, which could be explained by higher precipitation in these areas (Fig. 12) as well as higher topographic relief associated with the delineated sub-basins in this area (Fig. 5). It is also worth highlighting that Total and Dunne runoff coefficient, shown in Figs. 11 and 13 respectively, attained its peak in winter and were at its lowest in summer, which is attributed to opposite trend in PET estimates (Fig. 6) reaffirming the fact the seasonal variability in runoff coefficient is driven by the climatic forcing. Interestingly, Horton runoff coefficient (Fig. 15) was an order of magnitude less than Total and Dunne runoff coefficient. This can be attributed to the fact that in most humid and forested regions, as in the upland area of the Selke catchment (Fig. 1) where dominant landuse is a mix of coniferous and mixed forest, infiltration capacities are high because vegetation protects the soil from rain-packing and furthermore the activity of micro fauna create an open soil structure. Under these conditions, it is quite rare that infiltration capacities are ever exceeded by incoming precipitation consequently Horton overland flow is very infrequent.

In conclusion insights from this paper combined with the previous work of Jiang et al. (2014) can be of consequence and interest for the local stakeholders for designing and management of monitoring stations in the catchment. Finally, authors of the present work are aware that the work of similar nature have been published before, but as stated by (Ceola et al., 2015), reproducibility and repeatability of experimental as well as numerical work are the cornerstone for advancement of scientific knowledge in hydrology or any other scientific endeavour and it is in that spirit this analysis is presented.

Conflict of interest

We wish to confirm that there are no known conflicts of interest associated with this publication and there has been no significant financial support for this work that could have influenced its outcome. We further confirm that no other persons who satisfied the criteria for authorship but are not listed. The order of authors listed in the manuscript has been approved by all of us. We confirm that we have given due consideration to the protection of intellectual property associated with this work and that there are no impediments to publication, including the timing of publication, with respect to intellectual property. In so doing we confirm that we have followed the regulations of our institutions concerning intellectual property.
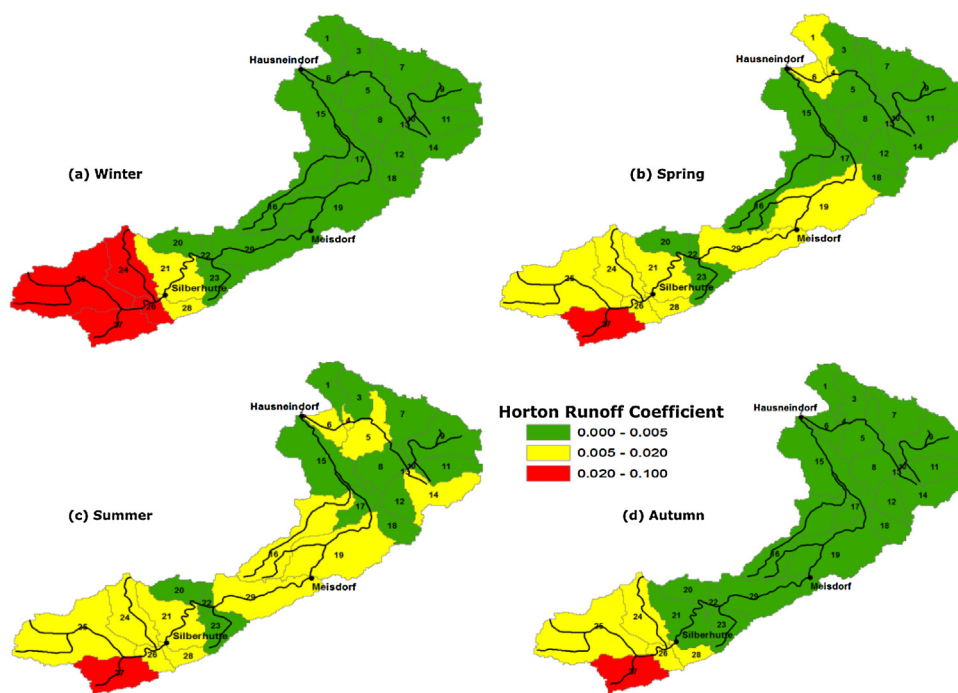
Acknowledgements

Fig. 15. Spatial variation of the Horton runoff coefficient with changing seasons.

Dr. Seifeddine Joma from Department of Aquatic Ecosystem Analysis from Helmholtz Centre for Environmental Research, UFZ, Germany for constructive discussion and sharing initial validation input files for the HYPE model

Appendix A. Supplementary data

Supplementary data associated with this article can be found, in the online version, at http://dx.doi.org/10.1016/j.ejrh.2016.06.002.

References

Al-Faraj, F.A.M., Al-Dabbagh, B.N.S., 2015. Assessment of collective impact of upstream watershed development and basin-wide successive droughts on downstream flow regime: the Lesser Zab transboundary basin. J. Hydrol., http://dx.doi.org/10.1016/j.hydrol.2015.09.074.

Anis, M.R., Rode, M., 2015. Effect of climate change on overland flow generation: a case study in central Germany. Hydrol. Process. 29, 2478–2490.

Arheimer, B., Lindström, G., 2013. Implementing the EU water framework directive in Sweden. In: Bloeschl, G., Sivapalan, M., Wagener, T., Viglione, A., Savenije, H. (Eds.), Runoff Predictions in Ungauged Basins – Synthesis Across Processes, Places and Scales. Cambridge University Press, Cambridge, UK, pp. 353–359, Chapter 11.20 (p. 465).

Arheimer, B., Dahné, J., Donnelly, C., Lindström, G., Strömqvist, J., 2011. Water and nutrient simulations using the HYPE model for Sweden vs. the Baltic Sea basin – influence of input-data quality and scale. Hydrol. Res. 43 (4), 315–329.

Arnold, J.G., Srinivasan, R., Muttiah, R.S., William, J.R., 1998. Large area hydrologic modeller and assessment part I: model development. J. Am. Water Resour. Assoc. 34, 73–89.

Benli, B., Bruggeman, A., Oweis, T., Ustun, H., 2010. Performance of Penman-Monteith FAO56 in a semiarid highland environment. J. Irrig. Drain. Eng. 136 (11), 757–765.

Bergstorm, B., 1992. The HBV model –its structure and applications. SMHI Reports RH, No. 4, Norrkoping.

Blaney, H.F., Criddle, W.P., 1950. Determining water requirements in irrigated areas from climatological and irrigation data, USDA (SCS) TP-96, 48 pp.

Ceola, S.E., Arheimer, B., Baratti, E., Blöschl, G., Capell, R., Castellarin, A., Freer, J., Han, D., Hrachowitz, M., Hundecha, Y., Hutton, C., Lindström, G., Montanari, A., Nijzink, R., Parajka, J., Toth, E., Viglione, A., Wagener, T., 2015. Virtual laboratories: new opportunities for collaborative water science. Hydrol. Earth Syst. Sci. 19, 2101–2117, http://dx.doi.org/10.5194/hess-19-2101-2015.

Clyde, G.D., 1931. Snow Melting Characteristics. Utah Agricultural Experiment Station Bulletin, pp. 231.

Collins, E.H., 1934. Relationship of degree-days above freezing to runoff. Transaction of American geophysical union, reports and papers. Hydrology, 624–629.

Doherty, J., 2005. PEST: Model Independent Parameter Estimation, User Manual, 5th ed. Watermark Numerical Computing, Brisbane.

Dunne, T., Leopold, L.B., 1978. Water in Environmental Planning. W H Freeman and Co, San Francisco, pp. 818.

Dunne, T., 1978. Field studies of hillslope flow processes. In: Kirby, M.J. (Ed.), Hillslope Hydrology. John Wiley, Chichester, U. K, pp. 227–293.

Freeze, R.A., 1980. A stochastic-conceptual analysis of a rainfall-runoff processes on a hillslope. Water Resour. Res. 16 (2), 391–408.

Garen, D., Moore, D.S., 2005. Curve number hydrology in water quality modeling: use, abuses and future directions. J. Am. Water Resour. Assoc. 41 (2), 377–388.

Gupta, H.V., Sorooshian, S., Yapo, P.O., 1999. Status of automatic calibration for hydrologic models: comparison with multilevel expert calibration. J. Hydrol. Eng. 4, 135–143, http://dx.doi.org/10.1061/(ASCE)1084-0699.

Hartmann, A., Wagener, T., Rimmer, A., Lange, J., Brielmann, H., Weiler, M., 2013. Testing the realism of model structures to identify karst system processes using water quality and quantity signatures. Water Resour. Res. 49, 3345–3358, http://dx.doi.org/10.1002/wrcr.20229.

Horton, R.E., 1933. The role of infiltration in the hydrologic cycle. Trans. Am. Geophys. Union 14, 446–460.

James, A.L., Roulet, N.T., 2009. Antecedent moisture conditions and catchment morphology as controls on spatial patterns of runoff generation in small forest catchments. J. Hydrol. 377, 351–366, http://dx.doi.org/10.1016/j.jhydrol.2009.08.039.

Jiang, S., Jomma, S., Rode, M., 2014. Modelling inorganic nitrogen leaching in nested mesoscale catchments in central Germany. Ecohydrology 2014, http://dx.doi.org/10.1002/eco.1462.

Kirchner, J.W., 2003. A double paradox in catchment hydrology and geochemistry. Hydrol. Processes 17 (4), 871–874, http://dx.doi.org/10.1002/hyp.5108.

Latron, J., Gallart, F., 2008. Runoff generation processes in a small Mediterranean research catchment (Vallcebre, Eastern Pyrenees). J. Hydrol. 358, 206–220.

Li, H., Sivapalan, M., Tian, F., 2012. Comparative diagnostic analysis of runoff generation processes in Oklahoma DMIP2 basins: the Blue River and the Illinois River. J. Hydrol. 418–419, 90–109.

Lindstrom, G., Johansson, B., Persson, M., Gardelin, M., Bergstrom, S., 1997. Development and testing of distributed HBV-96 hydrological model. J. Hydrol. 201 (1–4), 272–288.

Lindstrom, G., Pers, C., Rosberg, J., Stromqvist, J., Arheimer, B., 2010. Development and testing of the HYPE (Hydrological Predictions for the Environment) water quality model for different spatial scales. Hydrol. Res. 41 (3–4), 295–319.

McMillan, H., Gueguen, M., Grimon, E., Woods, R., Clark, M., Rupp, D.E., 2014. Spatial variability of hydrological processes and model structure diagnostics in a 50 km2 catchment. Hydrol. Processes 28, 4896–4913.

Moriasi, D.N., Arnold, J.G., Liew, M.W.V., Bingner, R.L., Harmel, R.D., Veith, T.L., 2007. Model evaluation guidelines for systematic quantification of accuracy in watershed simulations. Trans. ASABE 50, 885–900.

Nash, J.E., Suttcliffe, J.V., 1970. River flow forecasting through conceptual models part I –a discussion of principles. J. Hydrol. 10, 282–290, http://dx.doi.org/10.1016/00221694(70)90255-6.

Neupane, R.P., Kumar, S., 2015. Estimating the effects of potential climate and land use change on hydrologic processes of a large agriculture dominated watershed. J. Hydrol. 529, 418–429.

Pechlivanidis, I.G., Arheimer, B., 2015. 'Large-scale hydrological modelling by using modified PUB recommendations: the India-HYPE case'. Hydrol. Earth Syst. Sci. 19, 4559–4579, http://dx.doi.org/10.5194/hess-19-4559-2015.

Penna, D., Tromp-van Meerveld, H.J., Gobbi, A., Borga, M., Fontana, G.D., 2011. The influence of soil moisture on threshold runoff generation processes in an alpine headwater catchment. Hydrol. Earth Syst. Sci. 15, 689–702.

Razzaghi, F., Sepaskhah, A.R., 2010. Assessment of nine different equations for ETo estimation using lysimeter data in a semi-arid environment. Arch. Agron. Soil Sci. 56 (1), 1–12.

Reggiani, P., Sivapalan, M., Hassanizadeh, S.M., 2000. Conservation equations governing hillslope responses: exploring the physical basis of water balance. Water Resour. Res. 36 (7), 1845–1864.

Singh, V.P., 1997. Effect of spatial and temporal variability in rainfall and watershed characteristics on streamflow hydrograph. Hydrol. Processes 12, 147–170.

Spence, C., 2010. A paradigm shift in hydrology: storage thresholds across scales influence catchment runoff generation. Geogr. Compass 4 (7), 819–833, http://dx.doi.org/10.1111/j.1749-8198.2010.00341.x.

Tian, F., Li, H., Sivapalan, M., 2012. Model diagnostic analysis of seasonal switching of runoff generation mechanisms in the Blue River basin, Oklahoma. J. Hydrol. 418–419, 136–149.

Trom-van Meerveld, H.J., McDonnell, J.J., 2005. Comment to spatial correlation of soil moisture in small catchments and its relationship to dominant spatial hydrological processes. J. Hydrol. 303, 307–312.

Uhlenbrook, S., Mohamed, Y., Gragne, A.S., 2010. Analyzing catchment behaviour through catchment modeling in the gigel abay upper blue nile river basin. Ethiop. Hydrol. Earth Syst. Sci. 14, 2153–2165.

Vivoni, E.R., Entekhabi, D., Bras, R.L., Ivanov, V.Y., 2007. Controls on runoff generation and scale-dependence in a distributed hydrologic model. Hydrol. Earth Syst. Sci. 11, 1683–1701, http://dx.doi.org/10.5194/hess-11-1683-2007.

Walter, M.T., Shaw, S.B., 2005. Curve number hydrology in water quality modeling: use, abuses and future directions by David C. Garen and Daniel S. Moore. J. Am. Water Resour. Assoc. 41 (6), 1491–1492 (Discussion).

Western, A.W., Bloschl, G., Grayson, R.B., 1998. Geostatistical characterisation of soil moisture patterns in the Tarrawarra catchment. J. Hydrol. 205, 20–37.

Woods, R.A., Grayson, R.B., Western, A.W., Duncan, M.J., Wilson, D.J., Young, R.I., Ibitt, R.P., Henderson, R.D., McMohan, T.A., 2001. Experimental design and initial results from the mahurangi river variability experiment: Marvex. In: Lakshmi, V., Albertson, J.D., Schaake, J. (Eds.), Water Resources Monographs. American Geophysical Union, Washington, DC, pp. 201–213.

Yokoo, Y., Sivapalan, M., Oki, T., 2008. Investigation of the relative roles of climate seasonality and landscape properties on mean annual and monthly water balances. J. Hydrol. 357 (3–4), 255–269, http://dx.doi.org/10.1016/j.jhydrol.2008.05.010.

Zehe, E., Graeff, T., Morgner, M., Bauer, A., Bronstert, A., 2010. Plot and field scale soil moisture dynamics and subsurface wetness control on runoff generation in a headwater in the Ore Moauntains. Hydrol. Earth Syst. Sci. 14, 873–889.